

# PROCEEDINGS OF SPIE

[SPIDigitalLibrary.org/conference-proceedings-of-spie](https://spiedigitallibrary.org/conference-proceedings-of-spie)

## Attitude control system for a balloon based telescope

Jordi Vila Hernandez de Lorenzo, George Nehmetallah ,  
Stephen A. Rinehart

Jordi Vila Hernandez de Lorenzo, George Nehmetallah , Stephen A. Rinehart, "Attitude control system for a balloon based telescope," Proc. SPIE 10646, Signal Processing, Sensor/Information Fusion, and Target Recognition XXVII, 106461P (27 April 2018); doi: 10.1117/12.2304447

**SPIE.**

Event: SPIE Defense + Security, 2018, Orlando, Florida, United States

# Attitude Control System for a Balloon Based Telescope

Jordi Vila Hernandez de Lorenzo<sup>a,b</sup>, George Nehmetallah<sup>b</sup>, and Stephen A. Rinehart<sup>a</sup>

<sup>a</sup>NASA Goddard Space Flight Center

<sup>b</sup>EECS Department, The Catholic University of America

## ABSTRACT

The Balloon Experimental Twin Telescope for Infrared Interferometry (BETTII) is an 8-meter interferometer which operates on a high-altitude balloon. BETTII had its first successful engineering flight in June 2017.

In this paper we discuss the design of the control system for BETTII, which includes the coarse pointing loop and the estimator controls algorithm (Extended Kalman Filter) implemented in FPGA. We will also discuss the different system modes that we defined in the controls system loop, which are used in different phases of the flight and are activated in order to acquire a target star in the science detector. The pointing loop uses different sensors and actuators in each phase to keep pointing at the desired target. The main sensors are gyroscopes, star cameras, and auxiliary sensors such as high-altitude GPS and magnetometers. The azimuth control is achieved with Compensated Controlled Moment Gyros (CCMG) and a Momentum Dump motor. For the elevation control, high-precision motors are used, which change the elevation of the siderostat mirrors. The combination of these instruments keep the baseline oriented within few arcseconds from the target star.

In this paper, we will also present the software architecture relevant to the control system. This includes the description of the two flight computers present on the payload and the different control loops that are executed on them. Similarly, we will explain the importance of synchronization between all the sensors and actuators, which have to be referenced to a single master clock in order to obtain science data.

**Keywords:** Kalman Filter, Gyroscope, Star Camera, Field-programmable gate array (FPGA), Attitude control

## 1. INTRODUCTION

The BETTII payload is an 8-meter long boom interferometer, using a double-Fourier Michelson interferometer, to obtain far-infrared spectra of young stars in clustered star formation regions. BETTII provides a high angular resolution which will allow us to gather data on spectral energy distributions of individual deeply embedded protostars forming in dense clusters and distinguish between multiple embedded sources.

Space-based interferometric missions are crucial to the future of high resolution astronomy at infrared wavelengths<sup>1,2</sup> and BETTII is a balloon-borne pathfinder for future missions. The instrument is designed to achieve a spatial resolution of  $\sim 1''$  and a spectral resolution  $\lambda/\Delta\lambda$  of up to 100 in the Far Infrared (FIR) wavelengths (30 to 90  $\mu\text{m}$ ). Balloon experiments usually fly between 35 and 42km, above the 99.5% of the atmosphere, which make them particularly suited for studying the universe at infrared, far-infrared and sub-millimeter wavelengths.

During ascent, the temperatures can be as low as 213.15K (-60C). However, at float altitude the temperature stabilizes at around 233K (-40C), while the air pressure is 0.5% of the sea level pressure (about 5 mbar). Even though the air density is low, high altitude winds are still present, and large laminar flows move the balloon and payload as one. These disturbances excite pendulum motions which are typically of the order of a few arcminutes and have periods of a few to many tens of seconds. The control system is designed to cancel out these external perturbations with the actuators in azimuth, the Compensated Controlled Moment Gyros wheels (CCMGs), the momentum dump rotor and the actuators in elevation; the siderostat mirrors.<sup>3</sup> In order to produce interferograms both arms of the payload need to be pointed at the target. When the target is not exactly on-axis with the telescope, it can still fall on the detector as tip/tilt correction happens downstream. Hence, this requirement can be expressed as an overall pointing requirement of the instrument to some amount that can be corrected in

---

Author contact: Jordi Vila Hernandez de Lorenzo, [jordi.vilahernandezdelorenzo@nasa.gov](mailto:jordi.vilahernandezdelorenzo@nasa.gov)

tip/tilt in each individual arm. We set this to  $\pm 15''$  which roughly corresponds to one single pixel on the short band detector. Imposing this pointing requirement for the attitude control system we guarantee that the tip/tilt mechanisms will be able to align the target with the axis of the telescope.

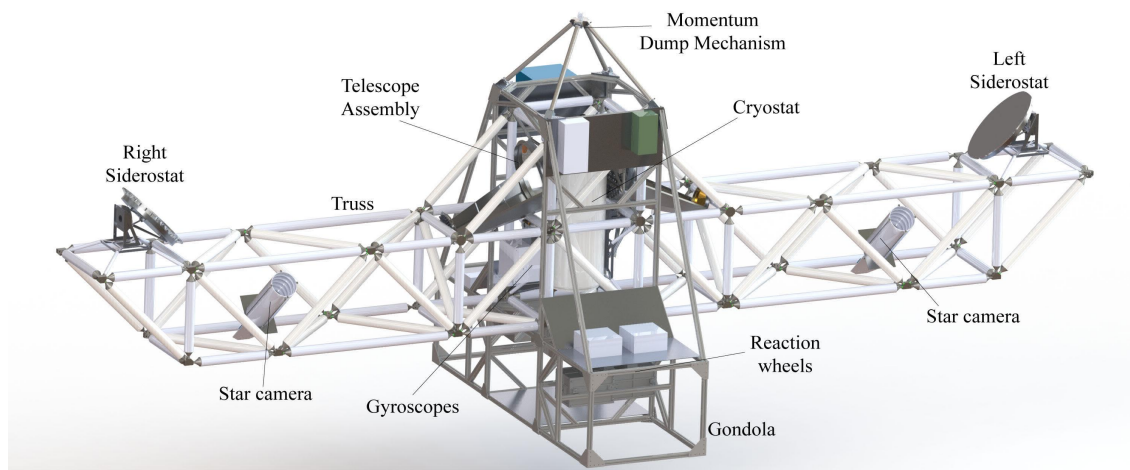


Figure 1: BETTII structural model showing the location of the different sensors.

The control system is designed to maintain the telescope pointing at a given target right ascension and declination celestial coordinates within the mentioned  $\pm 15''$  range. The absolute position orientation is determined thanks to the star camera and a finder software. This information is subsequently fed to the control loop that is executed in a Field-programmable gate array (FPGA). The control loop implements a Kalman Filter<sup>4</sup> which performs a set of rotations and estimations in order to determine the desired azimuth and elevation to which the actuators should be driven in order to capture the desired target. The desired positions for the various actuators in the gondola reference frame are achieved within the estimation loop, which runs at 100Hz and uses a set of PID controller gains that can be adjusted during flight.

At its fundamental level the control system has to be able to point the telescope at a given right ascension and declination. Ideally, the system needs to be able to achieve this goal autonomously. The pointing procedure moves the telescope at float and brings it from a random pointing location in the sky to pointing and tracking the desired science target. This procedure of moving the telescope requires several steps. To execute these steps, the control system has various modes of operation that will execute sequentially in order to acquire the desired target. Each mode has different configuration parameters on the control loop.

## 2. SENSORS

Numerous sensing and actuator subsystems are involved in order to point the telescope to the desired target star. This section discusses the core elements of the control system, which allow to precisely center any target star in the detector.

### 2.1 Star cameras

For redundancy, the attitude control system of BETTII has two star cameras, located approximately in the center of each arm. Knowing the angle of each star camera respect to the gondola reference frame is crucial for a proper Kalman Filter estimation. After precise measurements we determined that the left star camera was pointing at an angle of  $-46.87035705^\circ$  respect to the gondola reference frame, whereas the right star camera's elevation was of  $-44.96040461^\circ$ . The mounts that support both cameras have been specially-machined so they can withstand deformation due to the temperature gradients experienced during flight.

The star camera is triggered by one of the flight computers using a Transistor-transistor logic (TTL) pulse that corresponds to the start of a cycle in the estimation control loop. That way, we can match the future inertial solution obtained to a specific point in time, which will allow us to reconstruct the estimated position. Once the image is captured, it is sent to the other flight computer via a USB connection. That computer contains a C++ script that runs the finder software which processes the image. This script identifies blobs and matches the patterns in the picture to a database that contains a complete catalog of stars above a certain magnitude. Eventually the software solves the inertial orientation (RA, DEC and ROLL) of the image and provides the uncertainties of these three measurements. The original finder software had been developed by Cardiff University but during the launch campaign in Palestine, TX, we incorporated an alternative to camera solution finder software called Astrometry.net. Both codes were used seamlessly during BETTII's first flight in June 2017. From the ground computer we had the capability of switching which finder code to use, as well as to change multiple parameters of the cameras such as exposure time, minimum blob size or restricting the search area of the finder software in order to speed up the rate at which solutions can be found.

The lenses used provide low chromatic aberration, a wide field of view ( $10^\circ$ ) and a collecting area of  $90\text{mm}^2$ . However, they do not have an auto-focus mechanism built in. For this reason we specially designed and remotely operated an auto-focus mechanism consisting of a stepper motor a belt tensioner and a belt that grips to the lens. The belt tensioner maintains the tension on the belt regardless of the contractions and expansions caused by temperature changes during flight.

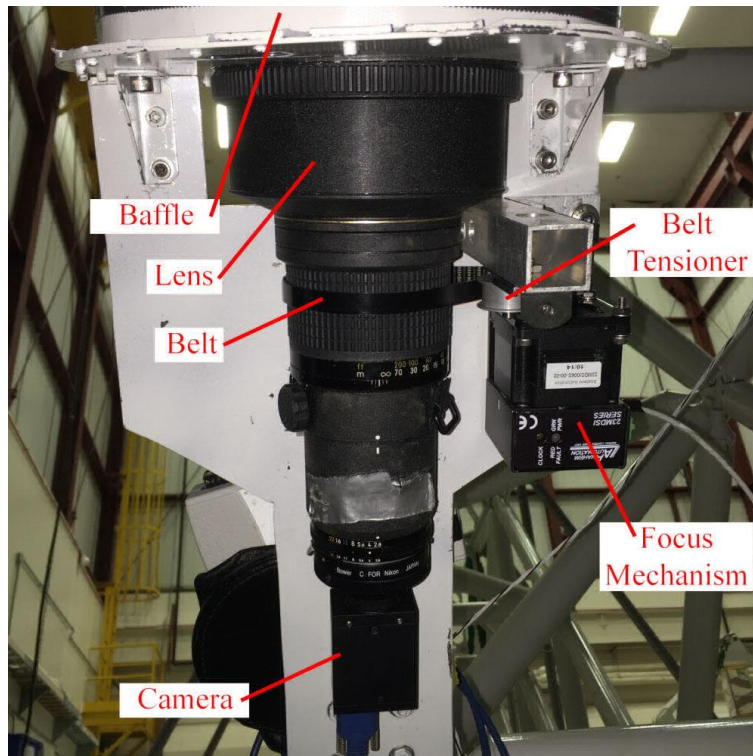


Figure 2: Star camera components

## 2.2 Gyroscopes

The three gyroscopes used to measure the angular velocity are from Optolink, the Latvian subsidiary of a Russian high tech company. We chose the SRS-2000 Sagnac model, which offer high precision and have very low angular random walk, thus adding little noise to each measurement. These gyroscopes are exceptionally good, if we integrate the gyroscope angular velocity measurement to obtain a position estimate, the estimation error we would make after one hour of integration would have a standard deviation of 2 arcseconds. The bandwidth

is 50Hz but they can be read up to 2kHz. Additionally, built-in thermal regulators maintain the temperature within a certain range in order to maintain precision when operating at different temperatures.

The three gyroscopes were mounted in an orthogonal configuration, however because the mount could not be orthogonal to the arcsecond level we had to apply a rotation matrix in the software in order to make the measurements perfectly orthogonal. By doing this cross correlations between different axes velocity measurements are avoided. Otherwise, that would have affected the pointing estimation.

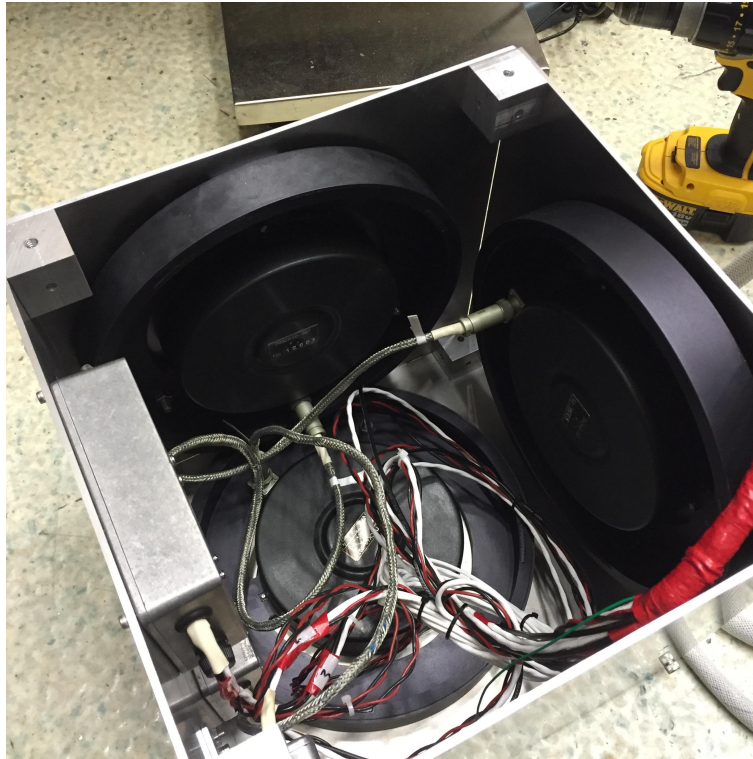


Figure 3: The SRS-2000 Optolink gyroscopes, mounted in an orthogonal assembly

### 3. ACTUATORS

The azimuth of BETTII is determined by the CCMGs and the Momentum Dump motor, whereas the elevation of the telescope is given by the angle of the two siderostat mirrors at the end of each arm.

We use three Galil Motion Controllers (DMC-4020) to control these 3 actuators. The first Galil controller maintains the rotation speed of the wheels. The second one controls the speed of the momentum dump motor as well as the angle of the rotation plane of the wheels. This rate of change of the rotation plane of the wheels will eventually determine the torque applied to the 2000lbs BETTII structure. The third Galil Controller commands the angle of the griffin motors that are attached to the siderostat mirrors.

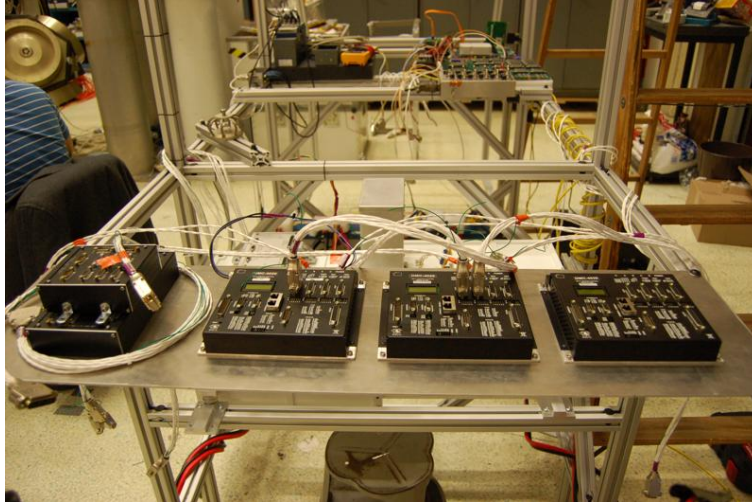


Figure 4: The Galil Motion Controllers command the CCMG wheels rotation speed, the gimbal angle, the momentum dump motor speed and the griffins angle.

Finally, the Tip/Tilt stage is responsible for adjusting the fine pointing and centering the target in the detector pixel array. The following sections will expand on all of these actuators.

### 3.1 Compensated Controlled Moment Gyroscopes Wheels (CCMG)

The CCMG features multiple encoders and motors, it consists of two counter-rotating reaction wheels attached to a gimbal stepper motor that changes the rotation axis of the wheels.

The wheels are spun by a brushless DC motor, their position is monitored with a relative 13-bit encoder that provides the wheels' positions. The exact location within a revolution is used within the control loop that maintains the wheels rotating speed of 50Hz. At power-up, the wheels start accelerating until they reach a constant speed of 3000 rpm in about 10 minutes. Similarly, the gimbal stepper motor is a Beckhoff AS1050 and it is also equipped with a 13-bit absolute magnetic encoder that provides the angle at which the wheels are rotating. Hard stops prevent the wheels from moving far past  $\pm 90^\circ$  from their nominal position.

At full speed the wheels spin at 3000 rpm and given its mass distribution it has been determined that at that speed they have a stored momentum of  $M_{CCMG} = 20.8$ . Note that, depending on the angle at which the wheels are rotating, the momentum along the z axis of the payload will vary. It is only the projection of this momentum vector on the z axis that will drive the effective torque on the payload.

$$M_{CCMG,z[Nms]} = 20.8 \times \sin\theta,$$

where  $\theta[\text{rad}]$  is the angle between the horizontal axis and the rotation axis of the wheels. If we think about it, when the rotation axis of the wheels is parallel to the z axis of the payload we have the maximum momentum, on the other hand, when the axes are orthogonal there is no momentum projected on the z axis of the payload. The Torque  $T_{CCMG}$  is the differential of the momentum with time.

$$T_{CCMG[Nm]} = \frac{d}{dt} M_{CCMG,z}$$

$$T_{CCMG[Nm]} = 20.8 \times \dot{\theta}_{[\text{rad s}^{-1}]} \cos\theta$$

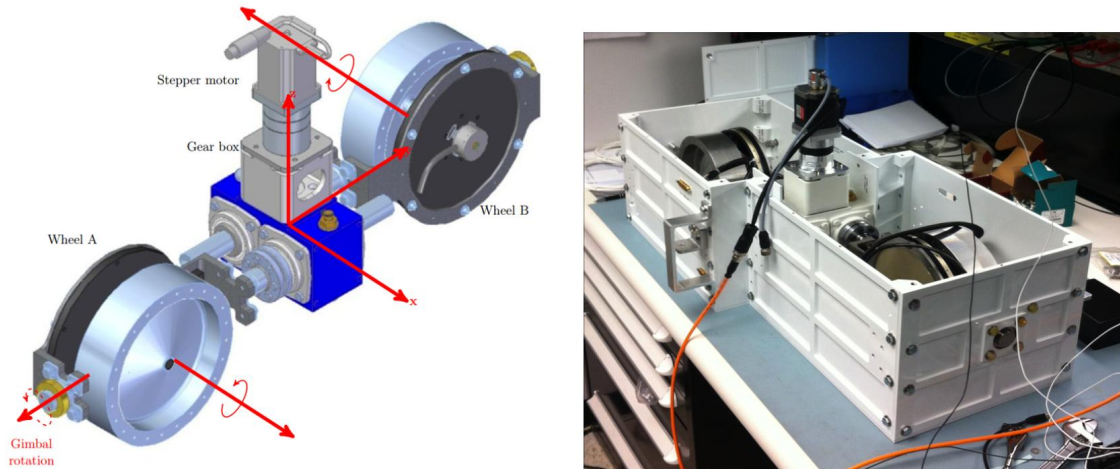


Figure 5: On the left we see a 3D model of the different parts of the CCMG assembly. The right picture shows the enclosing that also contains the gimbal stepper motor that adjusts the wheels' angle.

The change on the rotation axis angle directly impacts the torque. During operation we will always stay within a small range of angles, because at angles around 90 degrees the effect on the torque is practically nonexistent.

### 3.2 Momentum Dump

The function of the Momentum Dump motor is to maintain the wheels angle as close as possible to zero, thus, maximizing the available torque at any given time. This mechanism is attached to the balloon through a 100 foot ladder.



Figure 6: BETTII's launch. The momentum dump pin connects BETTII with the ladder and the parachute, which connects to the balloon

The principle behind the momentum dump is to rotate a motor that is connected via a double-bearing assembly to the pin that supports all the payload structure.

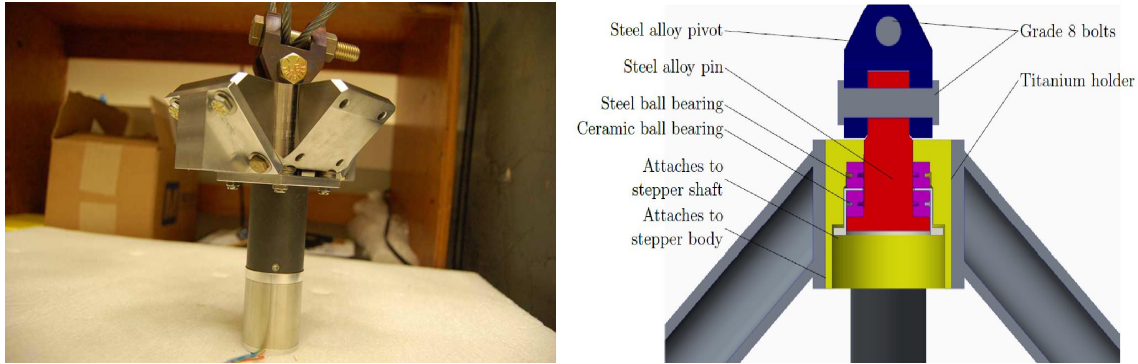


Figure 7: The pin that attaches to the balloon contains the stepper motor and the bearings to dump momentum to the balloon attachment assembly

The attitude control system controls the rotation speed of the momentum dump motor, which directly depends on the wheels' rotation axis angle and the inertia of the payload.

### 3.3 Siderostat mirrors

In order to reach the desired target, BETTII has to move in azimuth and elevation. The azimuth control is provided by the CCMG wheels and the momentum dump, whereas the elevation of the telescope is determined by the angle of the siderostat mirrors. The two siderostat mirrors have a diameter of 50 cm and are located in the edge of the truss. Theoretically, the angular resolution provided by the mirrors is about  $0.5''$  for the  $30\text{-}55\mu\text{m}$  band and  $1''$  for the  $55\text{-}110\mu\text{m}$  band. This resolution is much better than the existing telescopes that operate also in the far-infrared, which are limited by the mirror size. For reference, the James Webb Space Telescope will achieve the same resolution but for shorter wavelengths around the  $25\mu\text{m}$  band.

The rotators that control the angle of the siderostat mirrors need to operate at  $90^\circ$  from the gravity axis, they need to withstand temperatures as low as  $-40^\circ\text{C}$  and they need to have a precise encoder that allows not only smooth motion, but also accurate knowledge of the elevation angle. Griffin Motion LLC makes an industrial rotator that satisfies all of these conditions. The rotary encoder is an absolute encoder with 26bit resolution, which corresponds to a  $0.019''$  angular resolution.

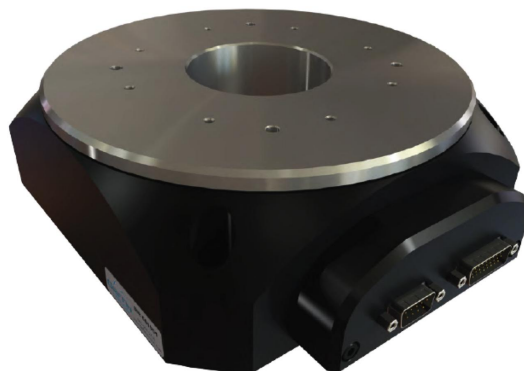


Figure 8: Rotation stages from Griffin Motion LLC.



### 3.4 Tip/Tilt stage

Finally, once the detectors have the observed target within a  $\pm 15''$  range, the last stage before acquiring the data is the centering of the target in the detector. For this fine pointing we use a tip/tilt mechanisms from Physik Instrumente. These actuators move a flat platform in tip and tilt planes and have a mirror attached to it. We put these mirrors close to a pupil of the optical system, to correct for angular errors. To achieve this goal the tip/tilt mirrors will center each beam with an accuracy of  $\pm 1''$  at the science detector.

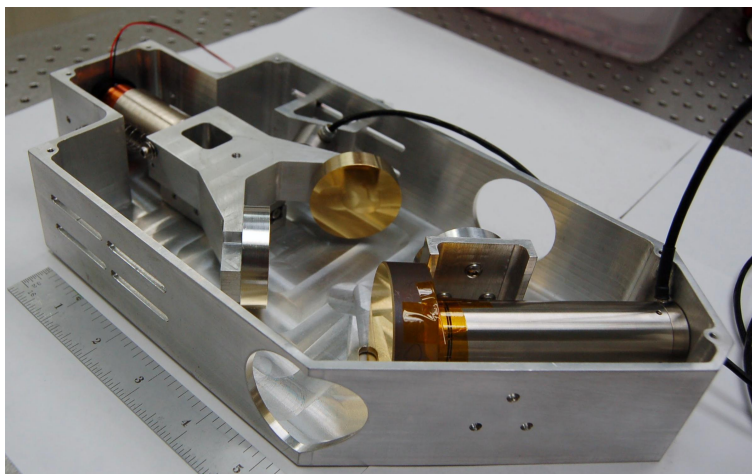


Figure 9: Tip Tilt platform used for coarse pointing

## 4. SOFTWARE ARCHITECTURE

The attitude control system of BETTII is based on an Extended Kalman Filter, which performs thousands of mathematical computations per second. To limit the the number of computations performed at each control loop cycle we use quaternions, which simplify rotations between the different reference frames. However, one of the complexities of the Kalman filter is that it involves inverting matrices to find the optimal solution when new absolute measurements are received. This has implications in terms of numerical complexity which often will limit the bandwidth of the filter, especially in the context of resource-limited FPGA computers on spacecraft. In practice the trade-off is the following: either limit the bandwidth of the filter, or limit the number of state parameters (i.e. limit the rank of the matrix to invert). On the ground, this limitation is usually not an issue. But even our powerful embedded computer will be limited in the speed at which it can find solutions.

### 4.1 Coordinate Systems

Stars can be located using the equatorial coordinate system, in terms of right ascension (RA) and declination (DEC) coordinates. This celestial coordinate system is useful because the stars are practically fixed in this frame, and they do not change their coordinates during the observation time. That does not occur if we use Azimuth and Elevation coordinates referenced to the Local Horizon plane. The star cameras will also provide solutions in this equatorial coordinate system and that is the reason why we will use it as our inertial reference frame to describe the attitude of the gondola. It is important to determine the inertial attitude in order to calculate the desired target's local azimuth Az and elevation El to which the gondola should point. Ideally, starting with only the targets location in RA and DEC, the system will be able to control the entire gondola to within  $15''$  of the target.

The Kalman filter is implemented in a cRIO, a computer that consists of an FPGA and a Real-Time operating system. To represent the attitudes and rotations of the different reference frames we use quaternions.<sup>5</sup> Briefly, quaternions extend the complex numbers and are very useful to describe three-dimensional rotations.

The goal is to estimate an attitude quaternion describing the inertial attitude of the gondola. In addition, we want to estimate the biases of the three gyroscopes to have better velocities measurements and improve our predictions. A Kalman filter will be used to obtain the estimate of these values.

The following picture describes the different reference frames used in the payload. Rotations between them are performed in the quaternion space and computed in the cRIO.

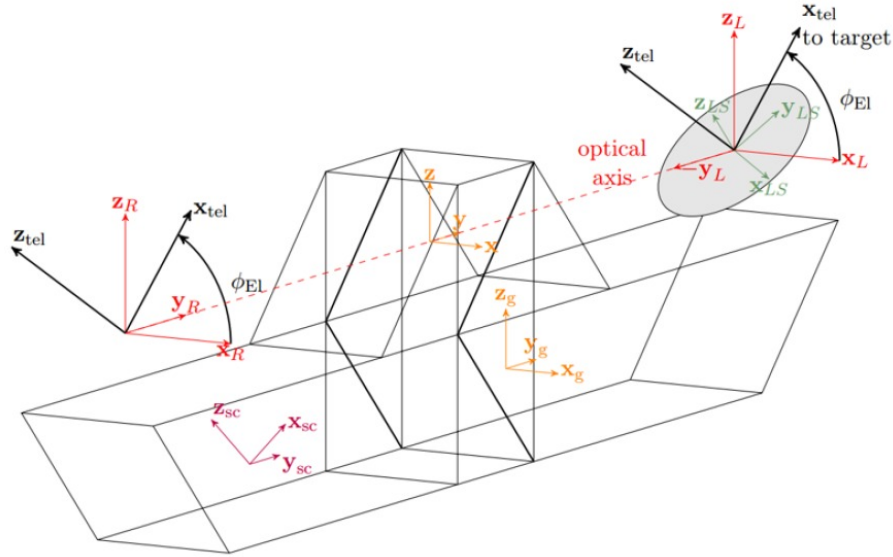


Figure 10: Coordinate systems relevant to the pointing control system. The subscripts sc, g, tel, L, R and LS indicate the star camera, gyroscope, telescope, left, right and left siderostat reference frames, respectively. The gyroscope reference frame is nominally aligned with the gondola reference frame, which has no subscript.

The attitude of BETTII is estimated using the information from the star cameras and the gyroscopes and the telescope is pointed using the CCMGs, the Momentum Dump motor and the Tip/Tilt stage. The information from the sensors is fused on an extended Kalman filter that will estimate the attitude and the gyroscopes biases. The starcameras typically provide pointing solutions every five seconds, whereas the gyroscopes are read at 100Hz. In case that the star cameras momentarily fail to find RA and DEC solutions, the system keeps integrating the gyroscopes velocities providing an accurate position measurement. However, if the star cameras were to permanently fail during flight, the Kalman filter software is designed to use a magnetometer and the GPS<sup>6</sup> information, including the local sidereal time, to provide an accurate pointing position within one degree. While these alternative instruments are not precise enough to achieve the arcsecond pointing level required to do carry our observations, they can be used to point the payload away from the sun, protecting the detectors and the electronics from overheating.

## 4.2 Computers

BETTII has two on-board computers, which we named Ford, in honor to the former First Lady of the United States Betty Ford, and Boop, in honor to the animated cartoon character Betty Boop.

Ford operates a real-time Linux kernel and is used to store all the data, process the up/down telemetry,<sup>7</sup> acquire star camera images, solve for inertial attitude, and process the science detector and H1RG frames. ford is an Adlink Extreme Rugged Express-IBR 3517UE with a dual-core i7 CPU and 4 GB of ECC (Error Checking and Correction) memory. The ECC memory is helpful in mitigating some of the side effects of cosmic ray hits on the memory chips. The computer has low power consumption, which allows it to function with a simple radiator instead of a fan. Prior to flight, Ford was successfully tested at in the environmental chamber, and the temperatures of its cores under maximum CPU stress have been monitored over long periods of time. During

flight, Ford's CPU registered internal temperatures as low as 0 °celsius, whereas the external temperatures were as low as -60 °celsius in the troposphere.

On the other hand, Boop is an FPGA and real-time computer from National Instruments to process the sensor input/outputs, implement the attitude estimation, and synchronize all the control loops. Boop is the brain of the control system. Boop is a National Instrument cRIO- system that features a reprogrammable FPGA chip in addition to a dual-core real-time operating system. NI LabView is the software interface to the system. Boop generates and distributes BETTII's master clock signal at 50 MHz.

The following table shows a summary of the various tasks performed by each computer:<sup>8</sup>

Name	Description & tasks
boop FPGA	<ul style="list-style-type: none"> <li>• Generate 50MHz master clock</li> <li>• Generate all other system clocks derived from master clock</li> <li>• Trigger all sensors</li> <li>• Read sensors: gyroscopes, galil controllers, ford at 100 Hz</li> <li>• Send actuator commands at 100 Hz</li> <li>• Implement hardware protection (limit, overdrive, etc)</li> </ul>
Boop RT	<ul style="list-style-type: none"> <li>• Collects all sensors from boopFPGA and estimate the inertial attitude and velocity</li> <li>• Create proper commands to all actuators and sends them to boopFPGA</li> <li>• Manages operating modes</li> <li>• Manages FIFOs and communication channels with ford</li> </ul>
Ford	<ul style="list-style-type: none"> <li>• Processes star camera frames to determine attitude</li> <li>• Processes science detector frames</li> <li>• Processes fine guidance sensor frames</li> <li>• Handles communication with the ground (through the CIP) and from/to boop</li> <li>• Automatically applies observing plan if no commands from the ground: send targets to boopRT</li> </ul>

Table 1: BETTII on-board computers.

### 4.3 Clocks and Timing

Due the nature of our instrument, we are very sensitive to vibrations across the structure, which could propagate throughout the payload and affect the data collected in the science detectors. All the undesired perturbations along the truss and the exoskeleton are introduced by the different sensors and actuators used to control BETTII. For instance, slight differences in the mass distribution of each of the two reaction wheels could create an undesired beat frequency that would affect our science data. If each wheel was driven by an independent clock, totally unsynchronized with the detector readout clock, it would be a challenge to retrieve the science data and the interferograms. Additionally, internal clocks tend to slightly drift with temperature changes, which would make it even harder to filter out the noise from the science data. For this reason, synchronization between all of the sensors and actuators across the payload has to be referenced to a single master clock, from which all the rest of clocks are derived. The master clock is a 50MHz TTL signal, generated using the high-precision internal electronics of the FPGA on the cRIO boop. In order to meet the detector readout rate requirements we have determined that the derived clock used by the control system has to have a frequency of 400.64Hz, which corresponds to a divider of 124,800 from the 50MHz master clock. This heartbeat drives the operations of some of the most critical processes:

- The Cold Delay Line (CDL) moves one single step
- The fine guidance sensor reads one single frame
- The science detector reads one single frame
- The CCMG wheel position about its axis is checked and a correction is applied.

A diagram of all the clocks in the system is shown in the following figure:

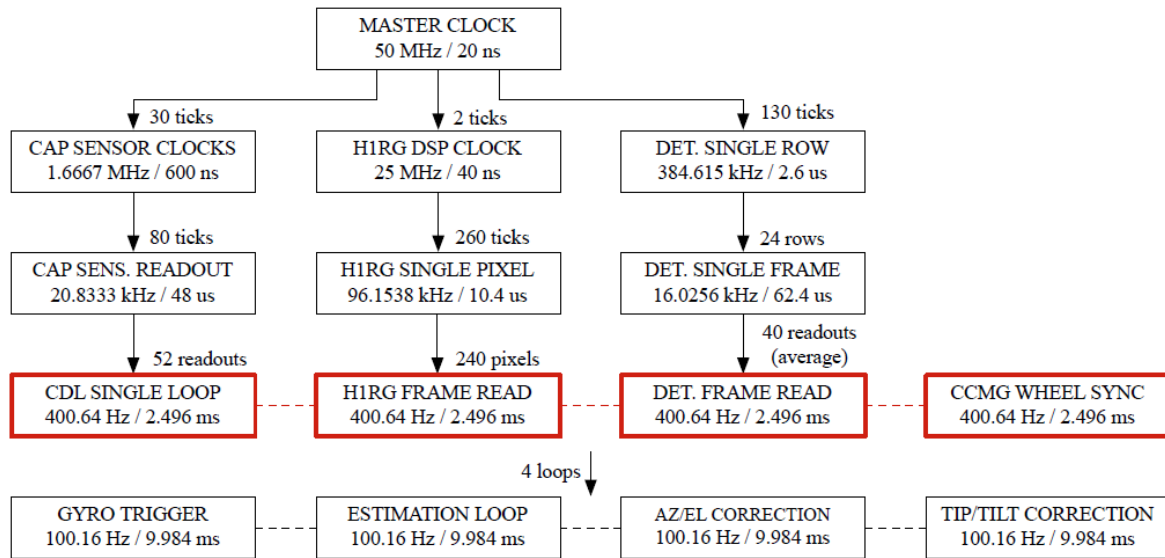


Figure 11: BETTII's clocks are all derived from one single master clock. The heartbeat at 2.496 ms is highlighted in red.

Following this implementation, a revolution of each single CCMG reaction wheel is set to be an integer multiple of this heartbeat, precisely 998,400 ticks, which is equivalent to  $8 \times 124,800$  master clock ticks (which is roughly equivalent to about 1 revolution every 20ms or 50 revolutions per second). Thus, every 8 heartbeats, each wheel is supposed to have rotated a full revolution. Similarly, the internal PID control loop of the CCMG controller adjusts the velocity of each wheel 8 times per revolution. This locks in the relative velocities of the wheels, which are now referenced to the same clock. Suppose now that a mechanical defect is present on the rotation point of the wheel that corresponds to the 8th heartbeat of a revolution. This small imperfection will cause a constant vibration frequency when the wheel is rotating along its axis. If we use a clock to control the wheels that is derived from the master clock, the generated vibration frequency is locked to our science data readout, such that we will see its effects every 8 data samples. If we think about this in the frequency domain, the undesired power peak is very sharp at a certain frequency and it is easy to filter, whereas the noise peak would be broadened if the clock frequencies were not synchronized. Besides, if the clocks were not synchronized and were drifting independently one from the other, a perturbation every eighth of a revolution would not necessarily affect one of every 8 detector samples. Thus, by synchronizing the clocks we can mitigate the perturbations introduced by unpredictable mechanical defects and independent clock drifts. Similarly, the control system output signals to the rest of the actuators are computed by the Kalman Filter and commanded to each motor every 4 heartbeats, which corresponds to 100.16 Hz or approximately 9.98 ms. Following this logic, not only the wheels, but all of our actuators are locked in with the master clock that sets the readout tempo of the science data. By using this clocking infrastructure we reduce the noise on the data and facilitate the data analysis process.

#### 4.4 Control Loops

For BETTII, each subsystem has its own PID control loop. Each PID loop structure consists of 7 parameters that can be adjusted from the ground: the  $K_p$ ,  $K_d$ ,  $K_i$  gains, and overall scaling factor, an upper and a lower limit on the command sent to the controller, and a boolean value that is used to reset the content of the integral term used to multiply  $K_i$ . The traditional PID loop can be enhanced in many ways to increase several of its properties, such as its robustness or noise-rejection properties. Given the reaction time of our actuators, we implement two key enhancements which are used in most of our PID loops. The first is a low-pass filtering of the derivative error, which helps avoid velocity noise (such as the structures resonant mode at 25 Hz) from being

injected into the command. The second is called a deadband, and is critical to the success of the azimuth loop that drives the stepper motor that controls the angle of the CCMG Wheels. Indeed, as the target is reached and the angular velocity has roughly a zero average, the velocity changes sign often due to its inherent noise. Since the proportional contribution is often small, this can cause the gimbal actuator to change direction very fast, which in turn excites vibrations, and contributes to wear on the stepper motor shaft. The deadband solves this problem by only using the derivative contribution if it is outside of a band about zero. This deadband is especially relevant when we are in the TRACK, ACQUIRE or LOCKED modes, which will be later on explored in greater detail. On BETTII, while this deadband makes the loop non-linear, its benefits far outweigh its drawbacks, especially since the deadband is typically kept at small values such as  $\pm 2'' s^{-1}$ .

A diagram showing the flow of the main loop of the control software is shown in the following figure.

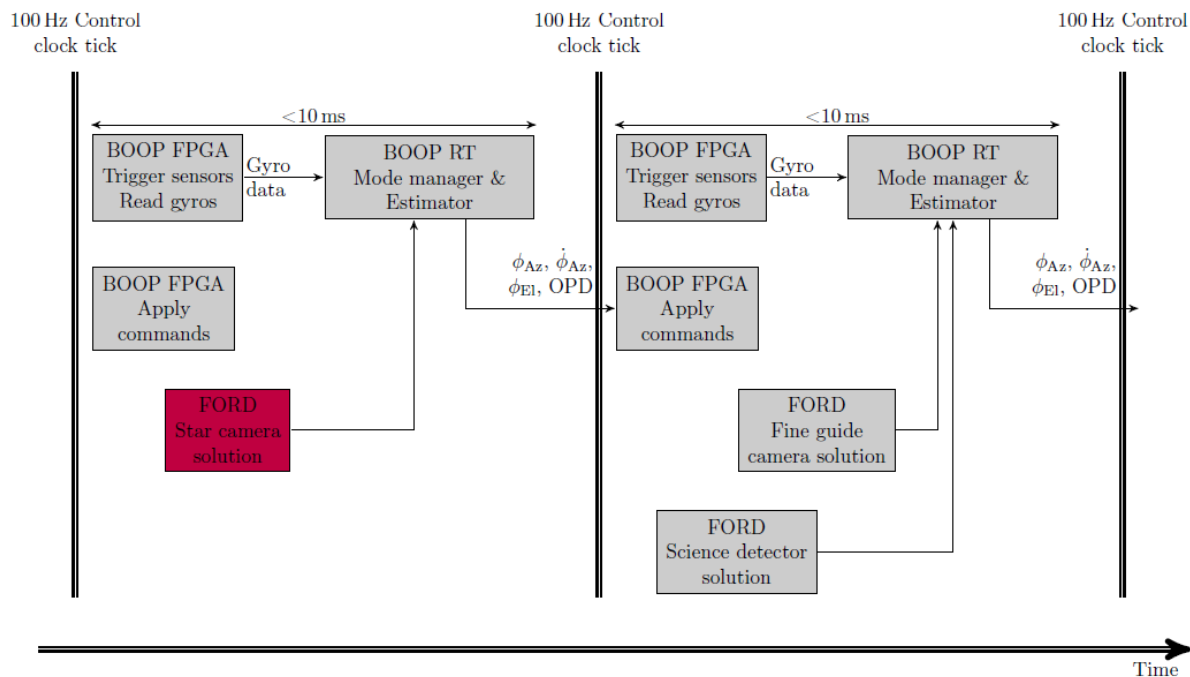


Figure 12: Two loops of the main control software. Right at each clock tick, the gyros are triggered in boop FPGA and read out. Once the sensors are triggered and read out, it triggers the loop in boop RT, which has then less than 10 ms to complete and send new commands back to the boop FPGA. These commands are not applied by the actuators until the next clock tick. This has the advantage to completely lock all moving parts of our payload to our heartbeat. The commands sent are using information from exactly 1 loop ago. This constant lag is preferred, as opposed to a scenario where the commands are applied as soon as possible, which would lead a variable lag which would depend on the processing time within boop RT.

This loop is operated at a nominal frequency of 100.16 Hz, which is the speed at which we read out the gyroscopes and issue new commands to the control system. The star camera, as well as other absolute sensors are being processed by the Real time software, and appropriately propagated since they often correspond to a measurement that was taken some number of loops ago. Using a robust synchronization scheme slaved to our systems master clock, we can align the various pieces of information with very high accuracy.

#### 4.5 Modes of operation

During flight, the payload will experience different environmental conditions, which require a different set of sensors and actuators to be active at each stage of the flight. This section summarizes the flight procedure for BETTII's flight from the launchpad to observation at 135,000 feet.

While rolling to the launchpad, during the balloon inflation and during ascent, BETTI is in SAFE mode, this means that all the PID gains of the control system are set to zero, allowing free movement of the gondola as it reaches the desired altitude, which is approximately two hours after launch. Once the turbulence from the ascent has died out, the control system determines where the gondola is currently pointing using the star cameras. For the software to process the star camera image, the payload has to be still to avoid blurring of the stars on the star camera sensor while the shutter is open (approximately 250ms). Hence, the first priority at this time of flight is to slow down the payloads inertial velocity, which is measured by the gyroscopes. Once the payload has stabilized, the star cameras are steady enough to take a picture of the sky where the stars will not be blurred and can be properly identified by the finder software. This procedure called BRAKE mode and its solely purpose is to slow down the azimuth velocity of the payload to a few arcseconds/s.

If the picture taken by the star camera is clear enough to detect blobs and stars, the system uses the camera frame to match the star patters to a known star data base stored on the flight computer Ford. With that, we can uniquely identify the inertial position of the payload. This triggers the estimator algorithm that constantly combines gyroscope and star camera information to determine the position every roughly 10ms. From this point on, we have a reasonable estimate of where the gyroscope reference frame is pointed with respect to the inertial frame. Thus, since we know the angle of the griffin mirrors, we automatically also know the orientation of the telescope in the inertial reference frame, that is, to which RA and DEC coordinates is the telescope pointing. When a new target in RA and DEC is set from the ground and sent up to the flight computers, the system will enter the SLEW mode. This creates a profile of desired azimuth position and velocity as a function of time. The software commands the reaction wheels to turn the payload about its z axis following these velocity and position profiles. These profiles create a smooth transition from any random position to the desired azimuth angle of the target that we want to observe, which could be as far as 180 degrees away from the current orientation of the payload. This profile is implemented to avoid a huge jump in the error signal that drives the azimuth control loop. The profile generates a velocity and position setpoint for each step of the control loop (10ms), which are fed to the proper actuators; the stepper motor that controls the rotation axis of the CCMG wheels and the momentum dump motor for the azimuth control, and the griffins angle for the elevation control. While the maximum azimuth acceleration of the payload is a constraint given by the mass distribution of the payload and the capabilities of the actuators, the maximum slew cruise velocity ( $V_{max}$ ) is a parameter that we can adjust from the ground, but is usually set around 1500 arcseconds/s. The following graph is an example of a calculated slew profile, where  $P_{target}$  stands for position target and to the azimuth projection of the desired star to be observed.

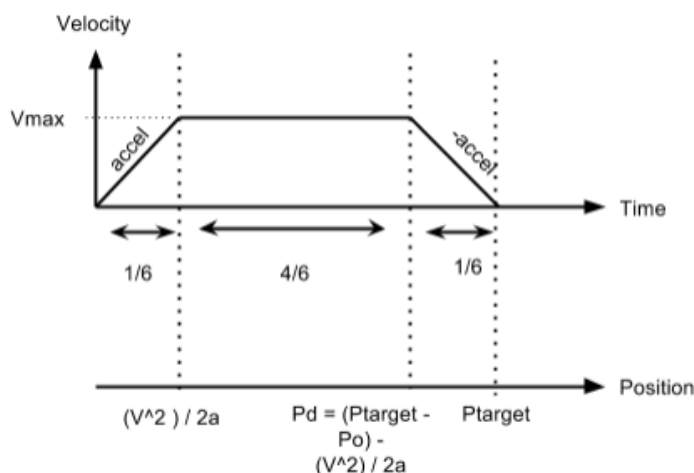


Figure 13: The Slew profile in velocity and position always has an acceleration stage which corresponds to 1/6th of the total slew time, a constant cruise period lasting 4/6 of the slew time and a deceleration phase taking the remaining 1/6th of the total time.

At the same time that the payload moves in azimuth, the control loop also commands the rotation stages that control the telescopes elevation. The control in elevation and control in azimuth are entirely decoupled but happen simultaneously. In fact, before the slew profile is completed, the system calculates at which elevation will the target to be observed be once the payload reaches the desired azimuth angle, and moves the siderostat mirrors at the proper elevation to start the observations as soon as the azimuth slew profile is completed.

When the deceleration phase is complete and the azimuth of the target has been reached, the system switches to TRACK mode. This mode tries to maintain control of the telescope within  $\pm 15''$  of the observed target. The TRACK mode requires small azimuth and elevation corrections, for this reason the PID gains that drive the actuators are completely different from the gains in other modes.

While in TRACK mode, the error signal fed to the PID control loop is the difference between the the azimuth position of the target and the current azimuth angle of the payload. If the magnitude of this error signal gets above a certain threshold, let's say due to an unexpected change of atmospheric conditions, the system automatically switches back to SLEW mode and approaches the target gradually, following, once again, a smooth slew profile.

Finally, for each of the two arms, we need to acquire a guide star onto our guide camera, this requires a fast imaging capability and a fast-steering tip/tilt correction mechanism to freeze the motion of the sky on the guide camera. This is ACQUIRE mode. Two images of the sky are made on the detector, one from each arm; the guide star is located in each image, and the tip/tilt mechanisms are actuated to center this star onto a location of the detector that corresponds to maximum overlap at the science detectors. Once the star is centered onto that location, the window size of the camera decreases, and the acquisition speed increases. Ultimately, we will get two patches of 3535 pixels at 50 Hz. When this acquisition speed is reached we consider ourselves in LOCKED mode. In both ACQUIRE and LOCKED mode, the position of the two tip/tilt platforms contains information on the overall mispointing of the optical train: when the actuators are both off in the same direction with respect to their nominal position, it means that the entire truss is off the guide star by this amount. When available, this information is used by the estimator along with the gyroscope and star camera information to compute the best possible attitude estimate. Since the tip/tilt is tied to the actual optics train, its information is heavily weighted compared to the other sensors.

Because light behaves like a wave, the intensity of the two light beams combined depends on the brightness of the source and the relative phase of each beam. Changes in this relative phase create a modulation of that intensity. This modulation is called an interferogram, which describes the measured intensity variation as a function of the phase difference between the two beams.

In order to produce interferograms, BETTII has two additional actuators, the warm delay line (WDL) and the cold delay line (CDL), which are also used in some of the modes of operation described above. The delay lines are a set of moving mirrors that introduce a path difference between the two beams of light. The warm delay line is outside the cryogenic chamber; its main goal is to center the interferogram and correct any optical delays caused, for example, by a residual misalignment of the telescope axis with respect to the source. The cold delay line has a ten times higher frequency control loop and is located inside the Dewar. It will generate a scan of optical path differences in order to obtain the desired interferogram.

While the CDL and the WDL are not used to point the telescope to the desired target, they are crucial to achieve the science results that we are seeking. The signals that drive the CDL and the WDL are generated in one of the control loops running in Boop.

These different modes of operation explained in this section are summarized in the following table:<sup>8</sup>

Mode	Description	Actuators	Sensors
SAFE	All PID gains set to 0; siderostats point towards zenith; azimuth is not commanded; used during ascent and emergencies	<ul style="list-style-type: none"> <li>• CDL</li> </ul>	<ul style="list-style-type: none"> <li>• Gyros</li> <li>• Star Cameras</li> </ul>
BRAKE	Used to slow down the payload after undesired motion; derivative gains only, no position loop	<ul style="list-style-type: none"> <li>• CDL</li> <li>• CCMG</li> <li>• Rotators</li> <li>• Mom. Dump</li> </ul>	<ul style="list-style-type: none"> <li>• Gyros</li> <li>• Star Cameras</li> <li>• Elevation encoder</li> <li>• Gimbal encoder</li> </ul>
SLEW	Used to move to target with a set velocity profile	<ul style="list-style-type: none"> <li>• CDL</li> <li>• CCMG</li> <li>• Rotators</li> <li>• Mom. Dump</li> </ul>	<ul style="list-style-type: none"> <li>• Gyros</li> <li>• Star Cameras</li> <li>• Elevation encoder</li> <li>• Gimbal encoder</li> </ul>
TRACK	Used to stabilize payload after slew, track target coarsely	<ul style="list-style-type: none"> <li>• CDL</li> <li>• CCMG</li> <li>• Rotators</li> <li>• Mom. Dump</li> </ul>	<ul style="list-style-type: none"> <li>• Gyros</li> <li>• Star Cameras</li> <li>• Elevation encoder</li> <li>• Gimbal encoder</li> </ul>
ACQUIRE	The guide camera grabs images for each arm and identifies the location of a guide star in increasingly smaller quadrant sizes	<ul style="list-style-type: none"> <li>• CDL</li> <li>• CCMG</li> <li>• Rotators</li> <li>• Mom. Dump</li> <li>• Tip/Tilts</li> <li>• WDL</li> </ul>	<ul style="list-style-type: none"> <li>• Gyros</li> <li>• Star Cameras</li> <li>• Elevation encoder</li> <li>• Gimbal encoder</li> <li>• Tip/Tilt encoders</li> <li>• Guide camera (H4RG)</li> </ul>
LOCKED	The intensity of the target in the science detector is measured, and the central phase is estimated	<ul style="list-style-type: none"> <li>• CDL</li> <li>• CCMG</li> <li>• Rotators</li> <li>• Mom. Dump</li> <li>• Tip/Tilts</li> <li>• WDL</li> </ul>	<ul style="list-style-type: none"> <li>• Gyros</li> <li>• Star Cameras</li> <li>• Elevation encoder</li> <li>• Gimbal encoder</li> <li>• Tip/Tilt encoders</li> <li>• Guide camera</li> <li>• Science detector</li> </ul>

Table 2: BETTII Operating Modes

## 5. CONCLUSION

In this paper, we have looked into the different sensors and actuators that form the control system of BETTII, an interferometer that flew in a balloon that was launched in June 2017 from the Palestine, Texas. The control system performance was successfully tested both in the lab at NASA Goddard Space Flight Center and in flight in June 2017, where we were able to demonstrate closed-loop pointing control of the payload. We also described the two flight computers that form the brain of BETTII; Boop and Ford, and explained the importance of proper synchronization between the different clocks and control loops running on the payload. Similarly, we explored the different modes of operation and how they are triggered to capture science data.

Currently the team is analyzing all of the data from the 2017 flight (over 1 terabyte), which includes extensive engineering and monitoring data and more than 250,000 H4RG detector images. The results of such analysis are expected to be published before June 2018 and will include details about the 2017 flight relevant to this paper, mainly related to pointing, timings and software performance but also related to power consumption, thermal monitoring and images captured by the H4RG detector.

The same team of scientists and engineers that built BETTII have started to develop BETTII2, which builds directly upon the development of the BETTII experiment, and incorporation of lessons-learned from BETTII will lead to improved scientific capabilities of the mission. The successful BETTII flight took a significant step



forward towards the system-level demonstration needed to pave the way for future space-based interferometers; BETTII2 will complete this demonstration and will provide valuable experience needed to develop the techniques for working with interferometric data. BETTII2 is expected to fly for the first time in 2020.

## REFERENCES

- [1] Leisawitz, D., Baryshev, A., Griffin, M. J., Helmich, F. P., Ivison, R. J., Rinehart, S. A., Savini, G., and Shibai, H., “Advancing toward far-infrared interferometry in space through coordinated international efforts,” (2013).
- [2] Kouveliotou, C., Agol, E., Batalha, N., Bean, J., Bentz, M., Cornish, N., Dressler, A., Figueroa-Feliciano, E., Gaudi, S., Guyon, O., Hartmann, D., Kalirai, J., Niemack, M., Ozel, F., Reynolds, C., Roberge, A., Straughn, K. S. A., Weinberg, D., and Zmuidzinas, J., “Enduring Quests-Daring Visions (NASA Astrophysics in the Next Three Decades),” *ArXiv e-prints* (Jan. 2014).
- [3] Veach, T. J., Rinehart, S. A., Mentzell, J. E., Silverberg, R. F., Fixsen, D. J., Rizzo, M. J., Dhabal, A., Gibbons, C. E., and Benford, D. J., “The balloon experimental twin telescope for infrared interferometry (BETTII): optical design,” in [*Optical and Infrared Interferometry IV*], *Proceedings of the SPIE* **9146**, 91462H (July 2014).
- [4] Trawny, N. and Roumeliotis, S., “Indirect Kalman filter for 3D attitude estimation,” University of Minnesota, Dept. of Comp. Sci. and Eng., Tech. (2005).
- [5] Breckenridge, W. G., “Quaternions - Proposed Standard Conventions. ech. rep. INTEROFFICE MEMORANDUM IOM 343-79-1199. NASA-JPL,” (1999).
- [6] uBlox, “u-blox M8 - Receiver Description and protocol specification,” Ublox (2017).
- [7] Vila Hernandez de Lorenzo, J., “Telemetry System of the Ballon Experimental Twin Telescope for Infrared Interferometry,” ISAE-SUPAERO (2014).
- [8] Rizzo, M. J., “BETTII: A pathfinder for high angular resolution observations of star-forming regions in the far-infrared.,” University of Maryland (2016).